The catalytic oxidation of aromatic hydrocarbons over supported metal oxide

Sang Chai Kim*

Department of Environmental Education, College of Engineering, Mokpo National University,
61 Torim-ri, Chungkye-myon, Muan-gun, Chonnam 534-729, South Korea

Abstract

The catalytic activity of metals (Cu, Mn, Fe, V, Mo, Co, Ni, Zn)/γ-Al$_2$O$_3$ was investigated to bring about the complete oxidation of benzene, toluene and xylene (BTX). Among them, Cu/γ-Al$_2$O$_3$ was found to be the most promising catalyst based on activity. X-ray diffraction (XRD), Brunauer Emmett Teller method (BET), electron probe X-ray micro analysis (EPMA) and temperature programmed reduction (TPR) by H$_2$ were used to characterize a series of supported copper catalysts. Increasing the calcination temperature resulted in decreasing the specific surface areas of catalysts and, subsequently, the catalytic activity. Copper loadings on γ-Al$_2$O$_3$ had a great effect on catalytic activity, and 5 wt.% Cu/γ-Al$_2$O$_3$ catalyst was observed to be the most active, which might be contributed to the well-dispersed copper surface phase. Using TiO$_2$ (anatase), TiO$_2$ (rutile), SiO$_2$ (I) and SiO$_2$ (II) as support instead of γ-Al$_2$O$_3$, the activity sequence of 5 wt.% Cu with respect to the support was γ-Al$_2$O$_3$ > TiO$_2$ (rutile) > TiO$_2$ (anatase) > SiO$_2$ (I) > SiO$_2$ (II), and this appeared to be correlated with the distribution of copper on support rather than with the specific surface area of the catalyst. The smaller particle size of copper, due to its high dispersion on support, had a positive effect on catalytic activity. The activity of 5 wt.% Cu/γ-Al$_2$O$_3$ with respect to the VOC molecule was observed to follow this sequence: toluene > xylene > benzene. Increasing the reactant concentration exerted an inhibiting effect on the catalytic activity. © 2002 Elsevier Science B.V. All rights reserved.

Keywords: Complete oxidation; Catalytic activity; Supported copper catalyst; BTX; Dispersion

1. Introduction

Volatile organic compounds (VOCs) are defined as hydrocarbons with a Reid vapor pressure of over 10.3 kPa at normal pressure and temperature, and recognized as major

* Tel.: +82-61-450-2781; fax: +82-61-453-4843.
E-mail address: gikim@chungkye.mokpo.ac.kr (S.C. Kim).

contributors to air pollution, either directly through their toxic or malodorous nature, or indirectly as ozone precursors and smog precursors [1]. These VOC contaminated gas streams are vented from a variety of industrial and commercial processes, such as printing, metal decorating, oil supplying, dry cleaning, paint drying, metal degreasing, manufacturing of organic compounds and polymers, and food processing, etc. The Clean Air Act Amendments of 1990 call for a 90% reduction in emissions of 189 toxic chemicals, 70% of them over the next 5 years [2]. In Korea, also, the ministry of the environment passed stringent legislation in 1999 that mandates industries with VOC emissions to install a facility to reduce them.

Catalytic oxidation is one of the most important and promising processes for VOC elimination, since catalytic incineration operates at temperatures much lower than those required for thermal incineration. The commercial catalysts for oxidizing VOCs can be classified into three categories: (1) supported noble metals [3,4]; (2) metal oxides or supported metals [5–7]; and (3) mixtures of noble metals and metal oxides [8,9]. In general, noble metal catalysts have greater activity than other metal catalysts, but their manufacturing cost is high.

The aim of the present work was to determine the most active metal/γ-Al$_2$O$_3$ catalysts for benzene, toluene and xylene (BTX) from the petrochemical industry as potential substitutes for noble metal-based VOC control catalysts, and to investigate the correlations between structure and reactivity for the most active metal and supports.

2. Experimental

2.1. Materials

Supported metal catalysts were prepared by the method of incipient wetness impregnation of γ-Al$_2$O$_3$, two different TiO$_2$ supports (rutile and anatase) and two SiO$_2$ supports with different surface areas, using the corresponding nitrate salts for Cu, Mn, Fe, V, Mo, Co, Ni and Zn as precursor compounds. The support was crushed, then sieved through 150–200 mesh. All precursor compounds and supports were obtained from Aldrich Products, except for γ-Al$_2$O$_3$ and SiO$_2$, which were obtained from Asian Catalyst. Impregnated supports were dried at 120 °C overnight. The dried material was then placed in a crucible for calcination. The material was heated to 400 °C, calcined for 2 h, then heated again to 700 °C, and calcined for 4 h in air. Also, the materials were calcined at 400, 500 and 600 °C for 6 h in air, respectively, to prepare the catalysts with different calcination temperatures. The metal content of the metal/γ-Al$_2$O$_3$ series was 15 wt.% and the copper content of the Cu/γ-Al$_2$O$_3$ series varied from 1 to 100 wt.%.

2.2. Experimental apparatus and procedures

A schematic diagram of the experimental apparatus is shown in Fig. 1; a conventional fixed bed flow reactor in the shape of a Y was employed. Mass flow controllers (UNIT Instrument, UFC-8100) were used for accurate and stable control of gas flow rates. Product and reactant analysis were carried out by a gas chromatograph (Shimadzu 14A) equipped with thermal conductivity. A Porapak Q column (50–80 mesh, 3 mm $\Phi \times$ 3 m) was used for CO$_2$ separation, and a 5% bentone-34, 5% DNP/shimalite column (60–80 mesh, 3 mm
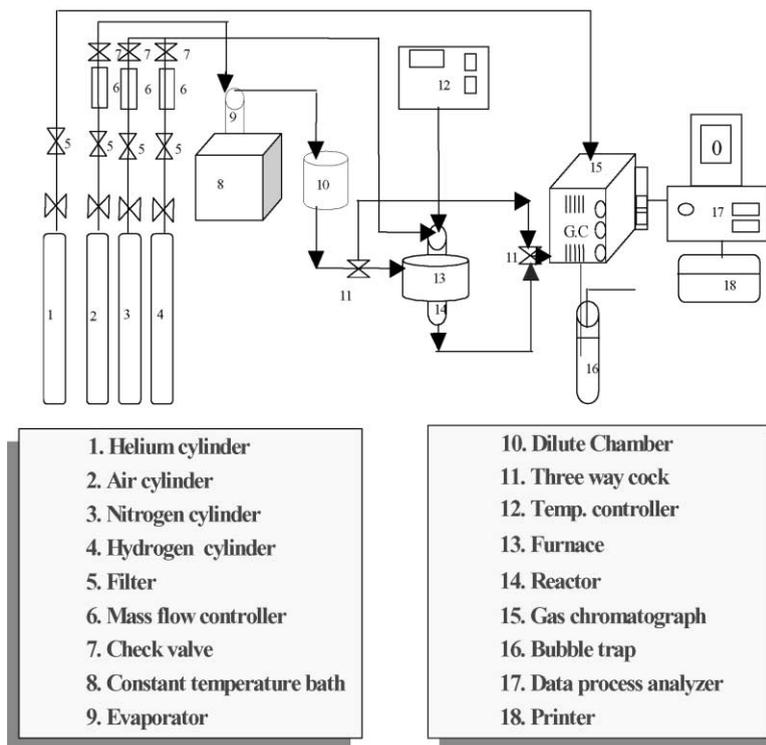
1. Helium cylinder	10. Dilute Chamber
2. Air cylinder	11. Three way cock
3. Nitrogen cylinder	12. Temp. controller
4. Hydrogen cylinder	13. Furnace
5. Filter	14. Reactor
6. Mass flow controller	15. Gas chromatograph
7. Check valve	16. Bubble trap
8. Constant temperature bath	17. Data process analyzer
9. Evaporator	18. Printer

Fig. 1. Schematic diagram of experimental apparatus.

$\Phi \times 3$ m) was used for VOCs analysis. Characterization was also carried out by GC/MS (Shimadzu, QP5050). The only products were CO_2 and H_2O. Other by-products were not found under most experimental conditions. Thus, the conversion was calculated based on hydrocarbon consumption. A blank test was conducted without a catalyst. No activity was observed below 500 °C.

The reactor system consisted of a vertical tubular of 35 cm length controlled by a PID controller. The reactor itself was a quartz tube of 12 mm o.d., at the middle of which the catalyst bed was contained. The catalyst in the 0.5 g mass was placed in the reactor, supported by quartz wool. The reactions were performed at temperatures ranging from 200 to 350 °C. A thermocouple (K type) was positioned in the catalyst bed for accurate measurement of the catalyst temperature. All catalysts were pretreated with 50 cm^3/min flow rate of air at 200 °C for 1 h prior to reaction. All gas lines of the apparatus were heated continuously at 110 °C in order to minimize VOC adsorption on tube walls.

BTX were purchased from Fisher and used directly. Xylene was an *ortho*-isomer. An air stream bubbling through a saturator filled with liquid hydrocarbon carried an individual vapor. The concentrations ranged from 160 to 1400 ppm, as controlled by the temperature of the saturator and mixed with another air stream. The concentration was always confirmed by GC before and after the experiment. X-ray diffraction (XRD, Geigerflex, Rigaku), Brunauer

Emmett Teller method (BET, AVSA, ASAP2000, Micromeritics), scanning electron micrograph and electron probe X-ray micro analysis (SEM and EPMA, Shimadzu, EPMA1600) were used to determine the effect of calcination temperature and Cu loading on the chemical state, the specific surface area and the dispersion of copper supported. Temperature programmed reduction (TPR) by H_2 was performed. The sample weight was 50 mg for TPR analysis. The sample was pretreated at 200 °C for 1 h in 40 cm^3/min (STP) before reduction. The reduction gas was typically 10% H_2/He mixture flowing at 40 cm^3/min (STP). The heating rate was typically 10 °C/min.

3. Results and discussion

3.1. Effect of metals

To survey the most active catalyst among the 15 wt.% metal (Cu, Mn, Mo, Fe, V, Co, Ni, Zn)/γ-Al$_2$O$_3$, complete oxidation reactions of toluene were performed with 1000 ppm concentration in air having a 40 cm^3/min flow rate within the temperature range of 200–350 °C, and the conversion as a function of temperature is shown in Fig. 2. In the case of Co/γ-Al$_2$O$_3$ and Ni/γ-Al$_2$O$_3$ catalysts, the conversions was negligibly low at a reaction temperature of 290 °C, and it was less than 5% even at a reaction temperature of 350 °C. Zn/γ-Al$_2$O$_3$ catalyst showed no conversion at a reaction temperature of 350 °C. In the case of Fe/γ-Al$_2$O$_3$, V/γ-Al$_2$O$_3$ and Mo/γ-Al$_2$O$_3$ catalysts, the conversions were less than 20% at a reaction temperature of 290 °C, and 88.6, 58.1 and 43.6%, respectively, at a reaction temperature of 350 °C. They showed the mid-range catalytic activity in all catalysts. In the case of
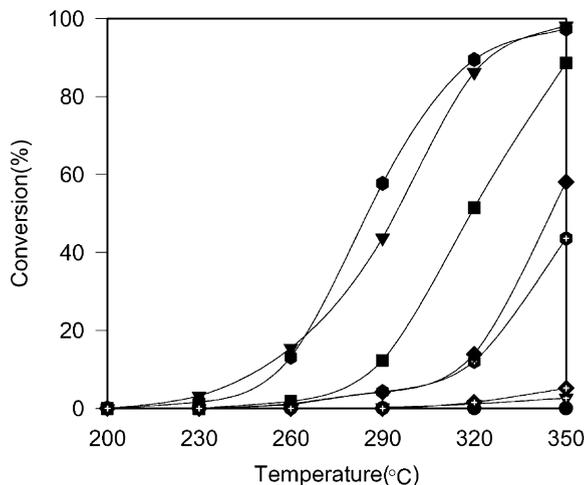

Fig. 2. Toluene conversion as a function of temperature on various metals catalysts. Reaction condition: catalyst weight = 0.5 g; toluene concentration = 1000 ppm in air; total flow rate = 40 cm^3/min; (●) 15 wt.% Cu/γ-Al$_2$O$_3$; (▼) 15 wt.% Mn/γ-Al$_2$O$_3$; (■) 15 wt.% Fe/γ-Al$_2$O$_3$; (◆) 15 wt.% V/γ-Al$_2$O$_3$; (⊕) 15 wt.% Mo/γ-Al$_2$O$_3$; (◆) 15 wt.% Co/γ-Al$_2$O$_3$; (▽) 15 wt.% Ni/γ-Al$_2$O$_3$; (●) 15 wt.% Zn/γ-Al$_2$O$_3$.

Cu/γ-Al$_2$O$_3$ and Mn/γ-Al$_2$O$_3$ catalysts, the conversions were 79.2 and 42.3%, respectively, at a reaction temperature of 290 °C and more than 98% at a reaction temperature of 350 °C. The activity of 15 wt.% metal/γ-Al$_2$O$_3$ with respect to metal was observed to follow the sequence: Cu > Mn > Fe > V > Mo > Co > Ni > Zn. As Cu/γ-Al$_2$O$_3$ appeared to be the most active catalyst, we focused on the supported copper catalyst system in the complete oxidation of VOCs.

3.2. Effect of calcinations temperature

It is known that the structure of Cu/γ-Al$_2$O$_3$ catalysts depends on both calcination temperatures and copper loadings [10–13]. Many research groups have reported a discrepancy in result between the structure of Cu/γ-Al$_2$O$_3$ and catalytic activity [14–18]. Fig. 3 shows the conversion as a function of temperature for complete oxidation of toluene over 15 wt.% Cu/γ-Al$_2$O$_3$ catalysts, prepared at different calcination temperatures. The conversions of 15 wt.% Cu/γ-Al$_2$O$_3$ catalysts calcined at 400 and 500 °C were 80.2 and 78.6%, respectively, at a reaction temperature of 290 °C and 98.5 and 97.4%, respectively, at a reaction temperature of 350 °C. In the case of calcination temperatures of 600 and 700 °C, the conversions were 63.2 and 57.5%, respectively, at a reaction temperature of 290 °C and 91.6 and 89.5%, respectively, at a reaction temperature of 350 °C. It was found that increasing the calcination temperature resulted in decreasing the conversion. XRD was used to determine the bulk crystalline phases in these catalysts. The diffraction patterns of the samples are shown in Fig. 4. It was observed that only CuO crystalline phases were present in the samples. BET measurements, results of which are summarized in Table 1, showed a higher surface area for 15 wt.% Cu/γ-Al$_2$O$_3$ prepared at lower calcination temperature, suggesting
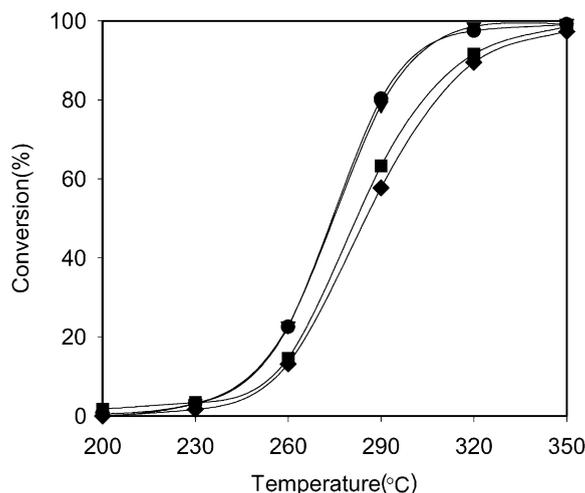

Fig. 3. Toluene conversion as a function of temperature on 15 wt.% Cu/γ-Al$_2$O$_3$ catalyst prepared at different calcination temperatures. Reaction condition: catalyst weight = 0.5 g; toluene concentration = 1000 ppm in air; total flow rate = 40 cm^3/min; (●) 400 °C; (▼) 500 °C; (■) 600 °C; (◆) 700 °C.
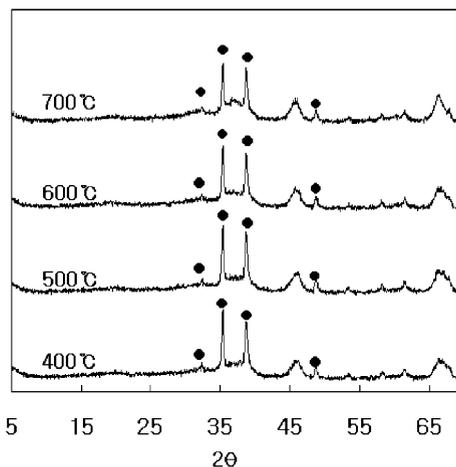
Fig. 4. XRD patterns measured for 15 wt.% Cu/γ-Al$_2$O$_3$ catalysts prepared at different calcination temperatures: (●) CuO.

a lower crystallinity. According to BET results, 15 wt.% Cu/γ-Al$_2$O$_3$ prepared at 700 °C of calcination temperature is the most crystalline phase. It appears that decreasing the conversion with increasing the calcination temperature is associated with decreasing the specific surface area, which can result in losing the active sites.

3.3. Effect of copper loading

The copper loadings of the Cu/γ-Al$_2$O$_3$ series varied from 1 to 100 wt.%. Fig. 5 shows the conversion as a function of temperature over these catalysts (1, 5, 10, 15, 100 wt.%). In the case of copper loading varied from 5 to 15 wt.%, the conversion decreased with increasing copper loadings. The conversions of 5 wt.% Cu/γ-Al$_2$O$_3$, 10 wt.% Cu/γ-Al$_2$O$_3$, and 15 wt.% Cu/γ-Al$_2$O$_3$, were 96.5, 94.7 and 92.8%, respectively, at a reaction temperature of 320 °C. In the case of copper (100 wt.%), the conversion was 81.9%. While the copper loading of the Cu/γ-Al$_2$O$_3$ was 1 wt.%, the conversion considerably decreased and was 29.2% at a reaction temperature of 320 °C. BET measurement results are summarized in Table 2. Increasing copper loadings resulted in decreasing the specific surface area. These results are in agreement with literature referring to carbon monoxide and methane oxidation [2]. As the conversions for copper loadings are volcano type, it does not seem that the conversion is

Table 1
BET surface area of 15 wt.% Cu/γ-Al$_2$O$_3$ catalysts

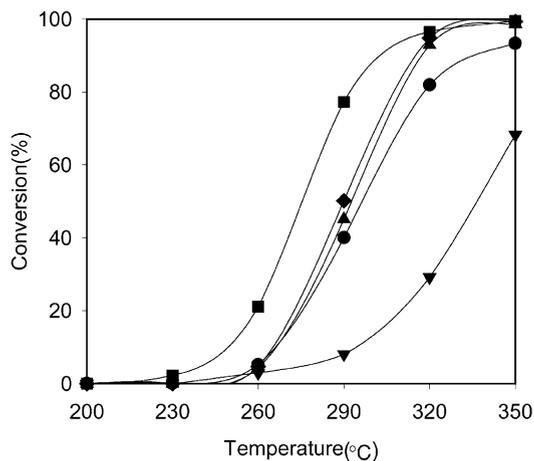| Catalyst	Calcination temperature of catalyst (°C)	Specific surface area (m^2/g)
15 wt.% Cu/γ-Al$_2$O$_3$	400	181.8
	500	179.3
	600	165.5
	700	157.5

Fig. 5. Toluene conversion as a function of temperature on different copper loadings on γ-Al$_2$O$_3$ catalysts. Reaction condition: catalyst weight = 0.5 g; toluene concentration = 900 ppm in air; total flow rate = 60 cm^3/min; ($\bullet$) Cu; ($\blacktriangledown$) 1 wt.% Cu/γ-Al$_2$O$_3$; ($\blacksquare$) 5 wt.% Cu/γ-Al$_2$O$_3$; ($\blacklozenge$) 10 wt.% Cu/γ-Al$_2$O$_3$; ($\blacktriangle$) 15 wt.% Cu/γ-Al$_2$O$_3$.

Table 2
BET surface area of different copper loadings on γ-Al$_2$O$_3$ catalysts

Catalyst	Specific surface area (m^2/g)
1 wt.% Cu/γ-Al$_2$O$_3$	210.0
5 wt.% Cu/γ-Al$_2$O$_3$	203.4
10 wt.% Cu/γ-Al$_2$O$_3$	198.4
15 wt.% Cu/γ-Al$_2$O$_3$	181.8
100 wt.% Cu	1.0
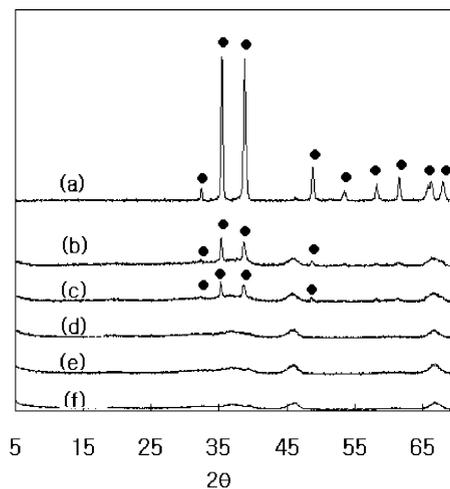
Fig. 6. XRD patterns measured for various catalysts: (a) Cu; (b) 15 wt.% Cu/γ-Al$_2$O$_3$; (c) 10 wt.% Cu/γ-Al$_2$O$_3$; (d) 5 wt.% Cu/γ-Al$_2$O$_3$; (e) 1 wt.% Cu/γ-Al$_2$O$_3$; (f) γ-Al$_2$O$_3$; ($\bullet$) CuO.

associated with the specific surface area. XRD patterns obtained for Cu/γ-Al$_2$O$_3$ with 5 wt.% Cu or lower showed only lines characteristic of the alumina support (Fig. 6). XRD patterns obtained for catalysts with higher copper loading ($\geq$10 wt.%) contained peaks characteristic of CuO (Fig. 6). The intensities of the CuO peaks increased with increasing copper loadings. These results indicate that for low copper loadings ($\leq$5 wt.% Cu on 211 m^2/g γ-Al$_2$O$_3$), copper is present as a well-dispersed surface phase. EPMA (right) and SEM (left) photographs of Cu/γ-Al$_2$O$_3$ catalysts are shown in Fig. 7. EPMA photographs also supported above results. The brighter the color, the higher the copper concentration in EPMA photographs. It was observed that copper on γ-Al$_2$O$_3$ might be highly dispersed for 1 and 5 wt.% Cu/γ-Al$_2$O$_3$ (Fig. 7a and b), but might not be for higher copper loadings ($\geq$10 wt.%) (Fig. 7c and d). Therefore, in the case of 1 wt.% Cu/γ-Al$_2$O$_3$, the lower activity is attributed to the insufficiency of active sites resulting from lower loading. The maximum toluene oxidation activity over 5 wt.% Cu/γ-Al$_2$O$_3$ can be attributed to the well-dispersed copper surface phase [14,17,18]. SEM photographs show that copper loadings have no effect on the morphology of the catalysts. TPR profiles of Cu/γ-Al$_2$O$_3$ catalysts with different copper
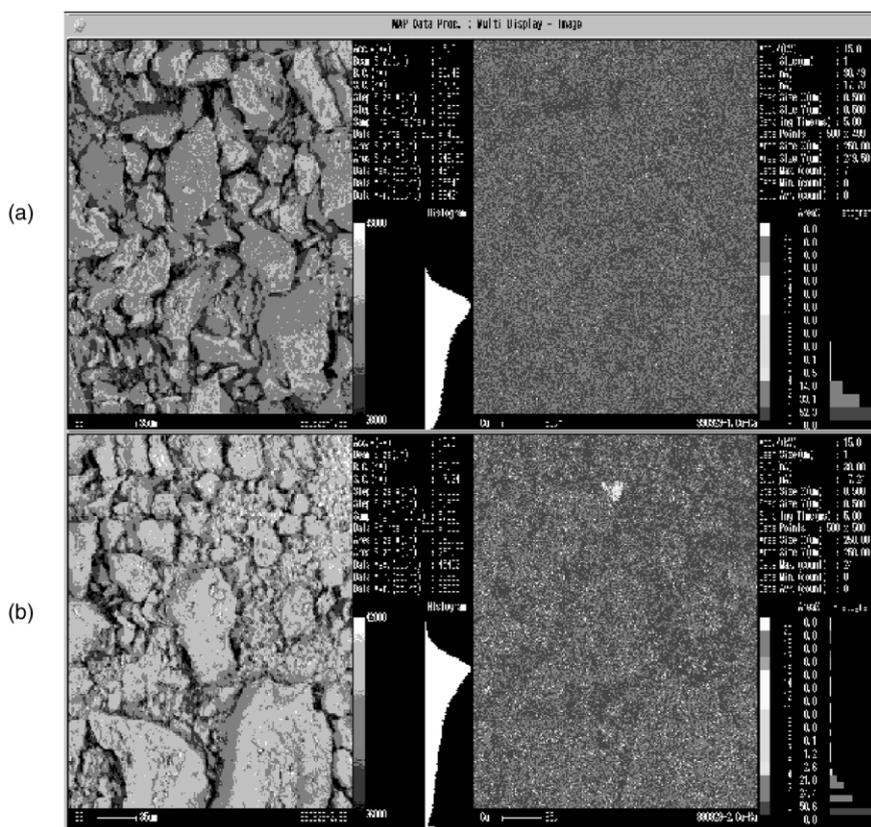

Fig. 7. EPMA photographs of various catalysts: (a) 1 wt.% Cu/γ-Al$_2$O$_3$; (b) 5 wt.% Cu/γ-Al$_2$O$_3$; (c) 10 wt.% Cu/γ-Al$_2$O$_3$; (d) 15 wt.% Cu/γ-Al$_2$O$_3$.
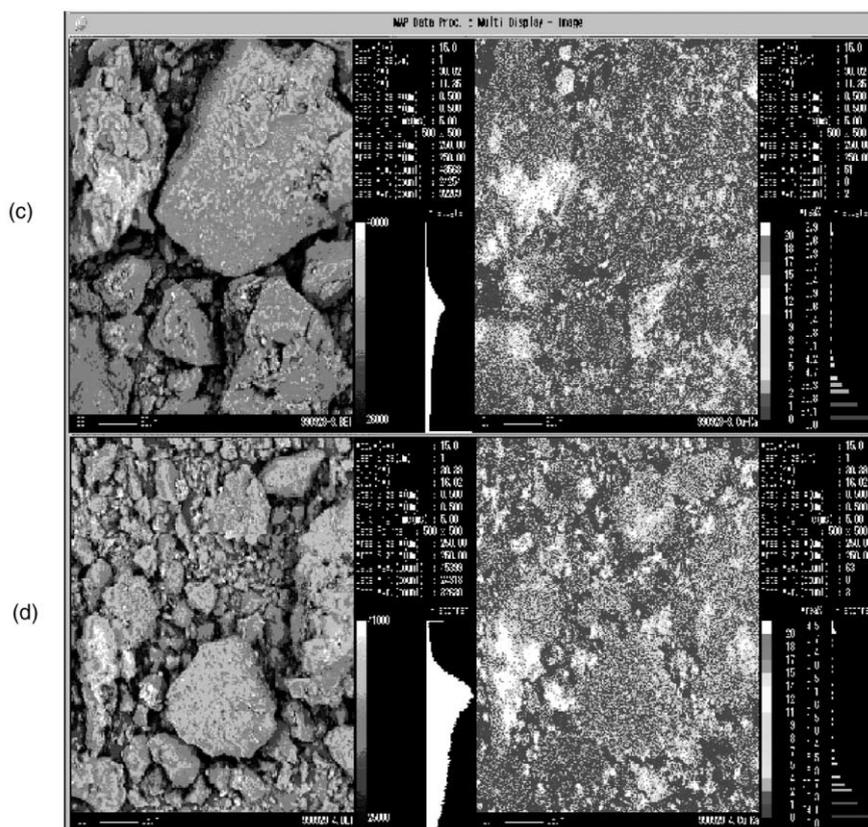
Fig. 7. (*Continued*).

loadings are shown in Fig. 8. The reduction profile changed significantly as the copper loadings increased. At least three different Cu species were revealed: 1 wt.% Cu/γ-Al_2O_3 gave no reduction peak; 5 wt.% Cu/γ-Al_2O_3 gave reduction peak with a maximum at ca. 250 °C; the reduction of 10 wt.% Cu/γ-Al_2O_3 consisted of a double peak whose maximum was at ca. 275 °C, while a smaller shoulder was observed at ca. 195 °C; in 15 wt.% Cu/γ-Al_2O_3, a large reduction peak was observed with a maximum at ca. 310 °C, while a much smaller shoulder was also observed at ca. 195 °C, and copper was mainly present as larger particles (Fig. 7d). Differences in the reduction profiles among catalysts with different copper loadings suggest that the state of the copper changes significantly as the copper loading changes. The observed reduction behavior may be attributed to structural differences. Kundakovic and Flytzani-Stephanopoulos [19] reported that at low copper loadings, copper is present as highly dispersed clusters or as isolated copper ions. Copper ions strongly interact with support, and reduction requires a temperature higher than 195 °C. These results suggest that copper is mainly present as isolated copper ions at 5 wt.%/γ-Al_2O_3, which are reduced with more difficulty than small copper clusters and more easily than bulk CuO, presenting at ca. 275 and 310 °C of maximum reduction peaks [19,20].
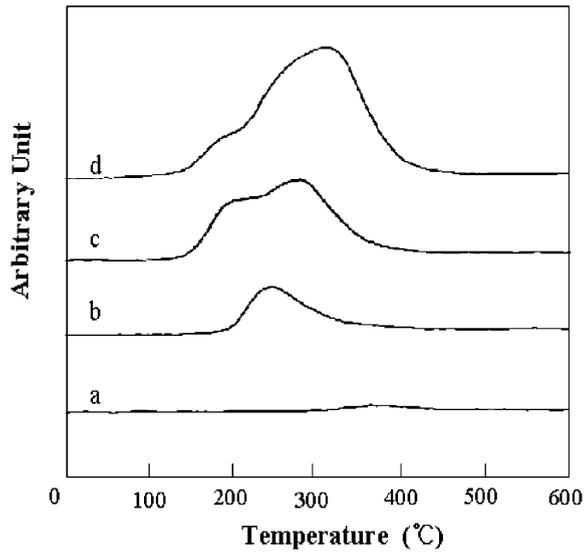
Fig. 8. TPR profiles measured for copper loadings catalysts: (a) 1 wt.% Cu/γ-Al$_2$O$_3$; (b) 5 wt.% Cu/γ-Al$_2$O$_3$; (c) 10 wt.% Cu/γ-Al$_2$O$_3$; (d) 15 wt.% Cu/γ-Al$_2$O$_3$.

3.4. Effect of supports

Fig. 9 shows the conversion as a function of temperature for the complete oxidation of toluene over 5 wt.% Cu with the supports such as TiO$_2$ (anatase), TiO$_2$ (rutile), SiO$_2$
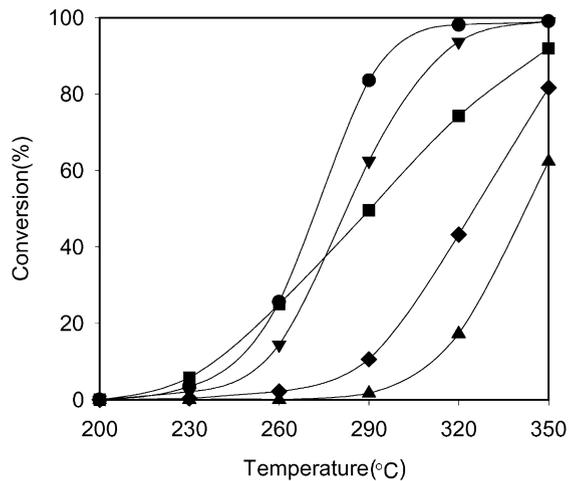

Fig. 9. Toluene conversion as a function of temperature on 5 wt.% Cu with various supports. Reaction condition: catalyst weight = 0.5 g; toluene concentration = 900 ppm in air; total flow rate = 40 cm^3/min; (▼) 5 wt.% Cu/TiO$_2$ (rutile); (■) 5 wt.% Cu/TiO$_2$ (anatase); (◆) 5 wt.% Cu/SiO$_2$ (I); (▲) 5 wt.% Cu/SiO$_2$ (II).

Table 3
BET surface area of 15 wt.% Cu with different support catalysts

Catalyst	Specific surface area (m^2/g)
5 wt.% Cu/γ-Al$_2$O$_3$	203.4
5 wt.% Cu/TiO$_2$ (rutile)	47.5
5 wt.% Cu/TiO$_2$ (anatase)	50.9
5 wt.% Cu/SiO$_2$ (I)	384.6
5 wt.% Cu/SiO$_2$ (II)	240.5

(I) and SiO$_2$ (II). The activity sequence of 5 wt.% Cu with respect to the support was γ-Al$_2$O$_3$ > TiO$_2$ (rutile) > TiO$_2$ (anatase) > SiO$_2$ (I) > SiO$_2$ (II). The results of the BET measurement are summarized in Table 3: 5 wt.% Cu/SiO$_2$ catalyst showed higher specific surface area, followed by 5 wt.% Cu/γ-Al$_2$O$_3$ and then 5 wt.% Cu/TiO$_2$ catalysts. The activity of 5 wt.% Cu with supports was found to be independent of the specific surface area of the catalysts. XRD patterns of samples are shown in Fig. 10. It was observed that CuO and TiO$_2$ crystalline phases were present in 5 wt.% Cu/TiO$_2$ catalysts, and CuO crystalline phases were present in 5 wt.% Cu/SiO$_2$ catalysts, which showed a higher crystallinity of 5 wt.% Cu/SiO$_2$ catalysts, and only lines characteristics of the alumina support in 5 wt.% Cu/γ-Al$_2$O$_3$. The higher the crystallinity, the greater the particle size of copper. EPMA (right) and SEM (left) photographs of these catalysts are shown in Fig. 11. SEM photographs show the morphology of the catalysts. EPMA photographs show that copper on γ-Al$_2$O$_3$ might be highly dispersed for 5 wt.% Cu/γ-Al$_2$O$_3$ (Fig. 10a), but might not be for copper loading on TiO$_2$ and SiO$_2$ (Fig. 10b and c). The sequence of copper dispersion degree with respect to supports was as follows: γ-Al$_2$O$_3$ > TiO$_2$ (rutile) > SiO$_2$ (I), results which were in agreement with the catalytic activity sequence. Different copper dispersions with respect to supports seems to be ascribed to strong metal-support interaction (SMSI), i.e. with
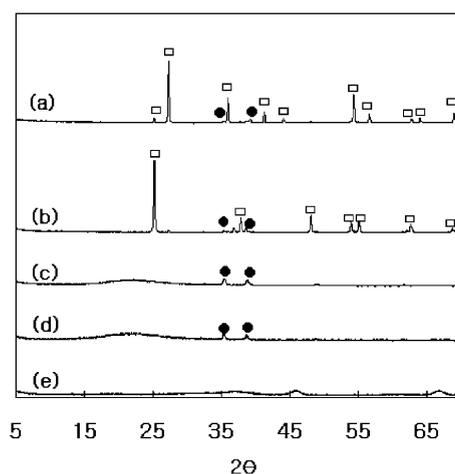

Fig. 10. XRD patterns measured for various catalysts: (a) 5 wt.% Cu/TiO$_2$ (rutile); (b) 5 wt.% Cu/TiO$_2$ (antase); (c) 5 wt.% Cu/SiO$_2$ (II); (d) 5 wt.% Cu/SiO$_2$ (I); (e) 5 wt.% Cu/γ-Al$_2$O$_3$; (●) CuO; (□) TiO$_2$.
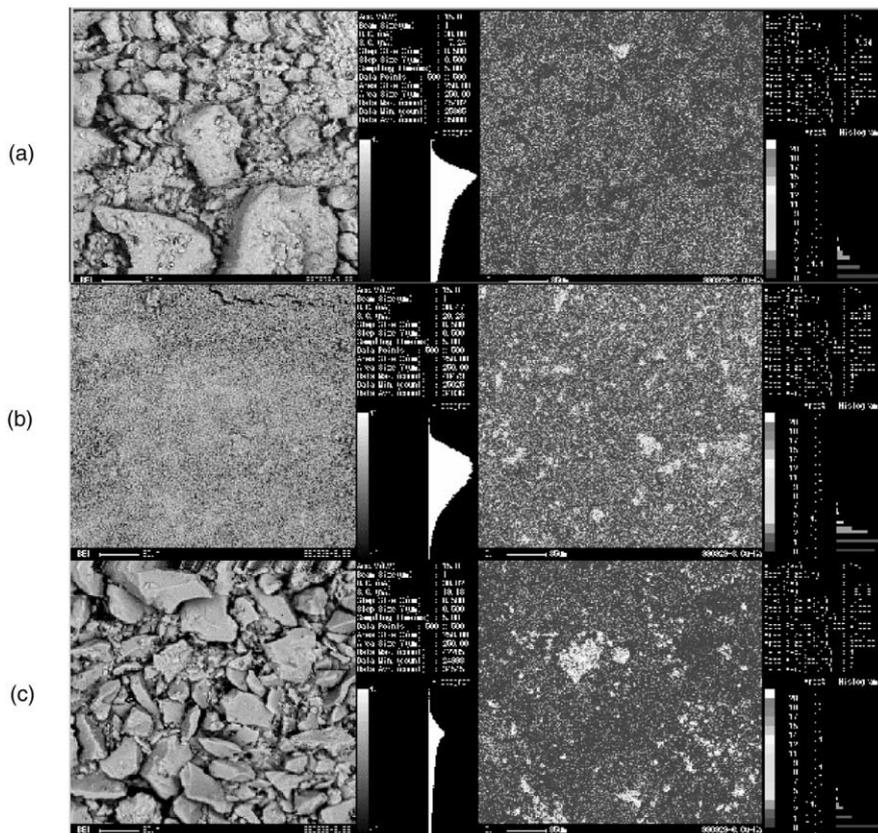
Fig. 11. EPMA photographs of various catalysts: (a) 5 wt.% Cu/γ-Al$_2$O$_3$; (b) 5 wt.% Cu/TiO$_2$; (c) 5 wt.% Cu/SiO$_2$.

increasing SMSI, the particle size of the metal decreases and, consequently, the surface area of the metal increases [21]. These results indicate that the smaller particle size of copper, due to its high dispersion on support, results in forming a copper surface phase and has a positive effect on catalytic activity.

3.5. Effects of reactant concentration and reactants

Fig. 12 shows the conversion as a function of temperature over 5 wt.% Cu/γ-Al$_2$O$_3$ catalyst, according to different toluene concentrations (160, 1000, 1400 ppm). For a toluene concentration of 160 ppm, the conversion was 100% at a reaction temperature of 290 °C; for 1000 ppm, 99.7% at a reaction temperature of 320 °C, and for a concentration of 1400 ppm, it was 98.2% at a reaction temperature of 350 °C. These results indicate that increasing reactant concentration results in decreasing activity. Such a phenomenon is normal for catalytic oxidation of VOC, i.e. the lower the concentration, the lower the light-off temperature [22].
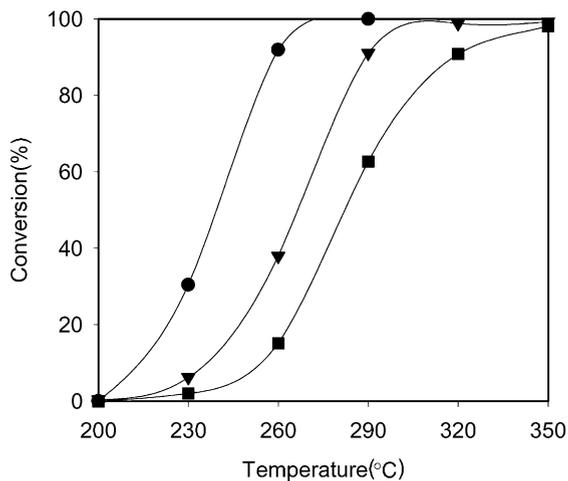
Fig. 12. Toluene conversion as a function of temperature at the different concentrations on 5 wt.% Cu/γ-Al₂O₃ catalyst. Reaction condition: catalyst weight = 0.5 g; total flow rate = 40 cm³/min; (●) 160 ppm; (▼) 1000 ppm; (■) 1400 ppm.

Wu et al. [23] reported that the activity of Pt/active carbon with respect to the VOC molecule was observed to follow the sequence: benzene > toluene > xylene, and the order of BTX activity followed the order of adsorption of BTX, indicating that the oxidation rate is correlated with the surface BTX concentration. Barresi and Baldi [24] reported that aromatics associated with the methyl groups over a Pt catalyst are more difficult to oxidize than benzene. However, as shown in Fig. 13, when each BTX was tested separately, this
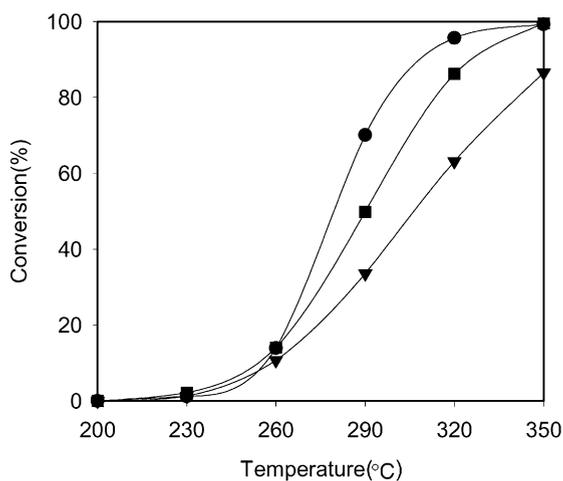

Fig. 13. BTX conversion as a function of temperature on 5 wt.% Cu/γ-Al₂O₃ catalyst. Reaction condition: catalyst weight = 0.5 g; BTX concentration = 800 ppm in air; total flow rate = 60 cm³/min; (▼) benzene; (●) toluene; (■) O-xylene.

activity sequence over 5 wt.% Cu/γ-Al$_2$O$_3$ was toluene > xylene > benzene. This activity sequence of toluene and xylene is consistent with that in previous literatures, but that of benzene is inconsistent. Becker and Förster [25] reported that compared with BTX were more reactive reactants because of the lower ionization potentials of the methyl derivatives. The ionization potentials of the methyl derivatives are 9.24 eV for benzene, 8.82 eV for toluene and 8.56 eV for xylene, therefore, benzene is the most difficult to oxidize. These results indicate that the combination of the catalyst property and the physicochemical property of the reactant plays an important role in activity.

4. Conclusion

1. Cu/γ-Al$_2$O$_3$ was found to be the most promising catalyst from the viewpoint of activity. Increasing the calcination temperature resulted in decreasing the specific surface areas of catalysts, subsequently the catalytic activity. The copper loadings on γ-Al$_2$O$_3$ had a great effect on catalytic activity, and 5 wt.% Cu/γ-Al$_2$O$_3$ catalyst was observed to be the most active.
2. Using TiO$_2$ (anatase), TiO$_2$ (rutile), SiO$_2$ (I) and SiO$_2$ (II) as support instead of γ-Al$_2$O$_3$, the activity sequence of 5 wt.% Cu/catalyst with respect to the support was γ-Al$_2$O$_3$ > TiO$_2$ (rutile) > TiO$_2$ (anatase) > SiO$_2$ (I) > SiO$_2$ (II), and it appeared to be correlated with the distribution of copper on support rather than with the specific surface area of the catalyst.
3. The activity of 5 wt.% Cu/γ-Al$_2$O$_3$ with respect to the VOC molecule was observed to follow the sequence: toluene > xylene > benzene, indicating that the combination of the catalyst property and the physicochemical property of the reactant plays an important role in activity.

Acknowledgements

References

[1] J.A. Horsley, Catalytica Environmental Report No. E4, Catalytica Studies Division, Mountain View, CA, USA, 1993.
[2] P.W. Park, J.S. Ledford, Appl. Catal. B: Environ. 15 (1998) 221.
[3] Z. Mingqian, Z. Bing, T.C. Karl, Appl. Catal. B: Environ. 13 (1997) 123.
[4] C.S. Jeffrey, T.Y. Chang, Catal. Today 44 (1998) 11.
[5] E.M. Cordi, P.J. O'Neill, J.L. Falconer, Appl. Catal. B: Environ. 14 (1997) 236.
[6] K.M. Parida, S. Amarendra, Appl. Catal. A: Gen. 182 (1999) 249.
[7] P. Papaefthimiou, T. Ioannides, X.E. Verykios, Appl. Catal. B: Environ. 13 (1997) 175.
[8] M.M.R. Peijen-Jeurissen, J.J. Jorna, B.E. Nieuwenhuys, G. Sinquin, C. Petit, J.P. Hindermann, Catal. Today 54 (1999) 65.
[9] S.K. Gangwal, M.E. Mullins, J.J. Spivey, P.R. Caffrey, B.A. Tichenor, Appl. Catal. 36 (1988) 231.

[10] A. Wolberg, J.F. Roth, J. Catal. 15 (1969) 250.
[11] G. Centi, S. Perathoner, D.B. Biglino, E. Giamello, J. Catal. 151 (1995) 75.
[12] R.M. Friedman, J.J. Freeman, F.W. Lytle, J. Catal. 55 (1978) 10.
[13] E. Garbowski, M. Primet, J. Chem. Soc., Chem. Commun. (1991) 11.
[14] F. Severino, J. Brito, O. Carias, J. Laine, J. Catal. 102 (1986) 172.
[15] J. Mooi, P.W. Selwood, J. Am. Chem. Soc. 74 (1952) 2461.
[16] E.D. Pierron, J.A. Rashkin, J.F. Roth, J. Catal. 9 (1967) 38.
[17] M.C. Marion, E. Garbowski, M. Primet, J. Chem. Soc., Faraday Trans. 86 (1990) 3027.
[18] M.C. Marion, E. Garbowski, M. Primet, J. Chem. Soc., Faraday Trans. 87 (1991) 1795.
[19] L.J. Kundakovic, M. Flytzani-Stephanopoulos, Appl. Catal.: Gen. 171 (1998) 13.
[20] W. Liu, M. Flytzani-Stephanopoulos, J. Catal. 153 (1995) 317.
[21] G.C. Bond, in: B. Imelik (Ed.), Metal Support and Metal Additive Effects in Catalysis, Elsevier, Amsterdam, 1982, p. 1.
[22] G. Veser, M. Ziauddin, L.D. Schmidt, Catal. Today 47 (1999) 219.
[23] J.C.S. Wu, Z.A. Lin, F.M. Tsai, J.W. Pan, Catal. Today 63 (2000) 419.
[24] A.A. Barresi, G. Baldi, Ind. Eng. Chem. Res. 33 (1994) 2964.
[25] L. Becker, H. Förster, Appl. Catal. B: Environ. 17 (1998) 43.